Title: Polyethylenimine Applications in CO2 Capture and Separation: from Theoretical Study to Experimental work

Authors: Xinhua Shen, PhD; Hongbo Du, PhD; Riley H. Mullins; Raghava Rao Kommalapati, PhD

To be cited as: 10.1002/ente.201600694

Link to VoR: https://doi.org/10.1002/ente.201600694

Polyethylenimine Applications in CO_2 Capture and Separation: from Theoretical Study to Experimental Work

Xinhua Shen, Hongbo Du, Riley H. Mullins, Raghava R. Kommalapati

Corresponding Author: Raghava R. Kommalapati

Abstract: The solid absorbents made with polyethyleneimine (PEI), which is loaded on different porous substrates, are promising for post-combustion CO_2 capture. The aim of this study is to review theoretical studies of polyamine applications including PEI on CO_2 capture and summarize the development of the experimental work of CO_2 capture using PEI. The mechanisms of CO_2 capture are discussed at different reaction suites of the polyamines, such as primary, secondary and tertiary amine groups. The experimental achievements CO_2 capture are investigated by the incorporation of PEI with different support materials, such as mesoporous silica and nanotubes, membranes and other materials such as alumina, zeolite, resin, metal organic frameworks, glass fibers, etc. through impregnation, grafting and synthesis. The excellent CO_2 capture capacity and great stability of PEI-impregnated nanomaterials display that PEI is one of the greatest candidates for CO_2 capture from flue gas or air.

1. Introduction

With the increasingly economical activities since the Industrial Revolution, anthropogenic carbon dioxide (CO_2) emissions, mainly coming from the combustion of carbon-based fuels, such as coal, oil and natural gas, cause the accumulation of CO_2 for more than two centuries on the earth. The increase of the global CO_2 concentration causes the greenhouse effects and is seriously concerned by most countries in the world. The Paris Agreement, which was the first-ever global climate deal, was adopted by 195 countries in 2015 under the framework of the United Nations. The agreement set out a global plan to limit the global average temperature increase to well below 2°C. Although different renewable and sustainable energies including hydropower, wind, solar, bio-, nuclear energies, etc. are broadly explored and used to reduce the emissions of the greenhouse gases (GHGs)[1], the carbon-based fuels will still be dominated in the industry in the next several decades mainly due to the economic efficiency. Prevention of the CO_2 emissions from power plants burning coal, oil and nature gas is seen as essential to mitigating the global greenhouse effects[2].

CO_2 capture and sequestration (CCS) from power plants is an effective strategy for the reduction of CO_2 emissions into the atmosphere[3]. Current technologies for CO_2 captures are generally classified into three approaches or processes: pre-combustion capture, oxy-fuel combustion and post-combustion capture[4]. These approaches or processes can be not only integrated into new power plants, but also applied to the retrofitting of existing power plants. Based on different fuel types and working conditions, each approach is chosen in practical applications. The pre-combustion capture is an economical option only when CO_2 concentration is higher and the pressure is higher in fuel feeding. Post-combustion capture can take more advantages for integrating into an existing power plant with continuous operation. Oxy-fuel combustion by using pure or higher concentration oxygen is the latest of the three approaches and is starting to apply for economical verification in factories. Typical technologies available for post-combustion capture are absorption (physical and chemical), adsorption and membrane separation[5]. Chemical absorption is more widely used than physical absorption due to its higher efficiency than the other. In chemical absorption, solvents such as amines, alcohols, ammonia solution, and alkaline solutions like NaOH, KOH, Na_2CO_3 and K_2CO_3 are employed. Solid adsorbents such as activated carbon, alumina, zeolites, metal organic frameworks, microporous carbon, polymers, polyamines, etc. are employed in adsorption.

Aqueous amine solutions such as mono- and diethanolamine (MEA and DEA) have been used to capture CO_2 and produce food grade CO_2 by the natural gas industry for more than 60 years[5a]. Aqueous amine absorption is feasible to capture CO_2 from gas streams with low CO_2 partial pressure. Due to corrosion and degradation issues, the MEA solution capture is operated in 15-20 wt% concentration for the Kerr-McGee/AGG Lummus Crest (KMALC) process and about 35 wt% concentration for the Fluor Econamine FG Plus^{SM} (EFG+) process[6]. The biggest issue of CO_2 capture in the aqueous phase is the high heat capacity of the amine solutions, causing high energy consumption and high cost during endothermic stripping/regeneration. Another big problem of aqueous amine absorption is the technical scalability, which limits its applications on CO_2 capture from common electricity power plants burning coal or natural gas. Other problems are equipment corrosion and amine solvent degradation caused by the oxygen present in aqueous solution.

CO_2 capture using solid adsorbents is considered one of the most promising technologies for CCS. To avoid the problems linked to the aqueous amine CO_2 capture, some solid amine adsorbents loaded with different support materials are intensively investigated and being developed. Different amine species have been explored to load on solid supports from the amine oligomers to amine polymers[7], such as MEA, DEA, diisopropylamine, tetraethylenepentamine (TEPA), dodecylamine, 3-aminopropyltriethoxysilane, tris(2-aminoethyl)amine, aziridine, poly(L-lysine), polyethylenimine

[a] Dr. Xinhua Shen
Department of Earth and Environmental Sciences
University of Northern Iowa
1227 W 27th St, Cedar Falls, IA 50614
E-mail: xinhua.shen@uni.edu
[b] Dr. Hongbo Du
Center for Energy & Environmental Sustainability
Prairie View A&M University
100 University Dr, Prairie View, TX 77446
E-mail: hodu@pvamu.edu
[c] Riley H. Mullins
Department of Earth and Environmental Sciences
University of Northern Iowa
1227 W 27th St, Cedar Falls, IA 50614
E-mail: mullinsr@uni.edu
[d] Dr. Raghava R. Kommalapati
Center for Energy & Environmental Sustainability, Department of Civil and Environmental Engineering
Prairie View A&M University
100 University Dr, Prairie View, TX 77446
E-mail: rrkommalapati@pvamu.edu

(PEI), etc.. These amines react with CO_2 through the presence of primary, secondary and/or tertiary amino groups.

Figure 1 shows the mechanisms of these amino groups reacted with CO_2[8]. Under dry condition, primary or secondary amines react with CO_2 to form carbamate, and may further convert to carbamic acid[8b, 8c] and/or bicarbonate at the secondary amine sites in the presence of water. Carbamic acid is dominated with high amine loading on substrate, and bicarbonate can be confirmed with low amine loading[8d]. The tertiary amines react with CO_2 only under humid condition. MEA, DEA and amine oligomers would have the similar problems of equipment corrosion and adsorbent degradation similar to solvent amine because of the instability of their small molecules. Therefore, in all the amines applied to solid absorbents, PEI is mostly investigated because it is easily synthesized, relatively cheap and more thermostable compared to MEA, DEA and amine oligomers.

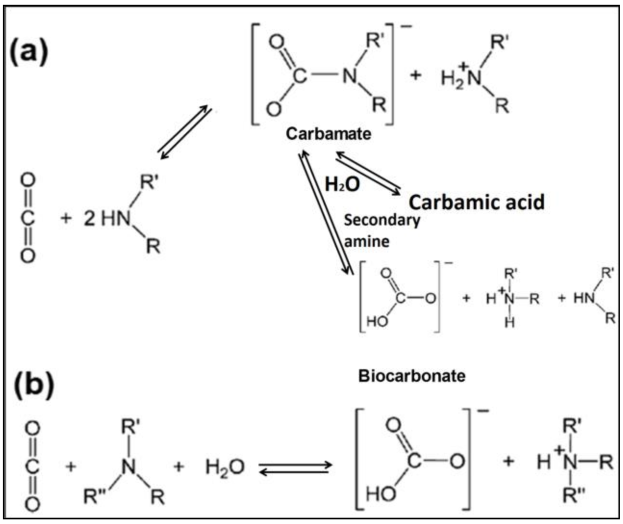

Figure 1. General mechanisms of primary (a), secondary (a) and tertiary (b) amines reacted with CO_2 (Adapted from Ref. 8).

PEI is a multi-purpose polymer with repeating units composed of one amine group and two carbon aliphatic CH_2CH_2 spacers and is widely used in many products, e.g., a wet-strength agent in cellulose paper industry, detergents, adhesives, water treatment agents and cosmetics[9]. There are three types of PEI polymers: linear, branched and dendrimer PEIs. Since PEI was first introduced in CO_2 capture in space shuttle by Satyapal et al.[10], many researchers have studied PEI as adsorbent for CO_2 captures by loading it on many support materials. Typical technologies for loading of PEI on support materials are impregnation, post-synthesis grafting, direct condensation[11] and copolymerization suitable for membrane separation[12]. In our review, we are focusing on PEI applications in CO_2 capture and separation studied from theories to experiments.

2. Theoretical Studies

Dr. Xinhua Shen is an Assistant Professor of Meteorology/Air Quality in the Department of Earth and Environmental Sciences at University of Northern Iowa. She completed her Ph.D. in Atmospheric Science at Colorado State University. Her research focuses on air quality measurement and modeling, cloud-aerosol-precipitation interactions, as well as air pollution control technologies including carbon capture with different nanomaterials.

Dr. Hongbo Du received his BS and Master degrees in mechanical engineering from Beijing Forestry University, China, and Ph.D. degree in mechanical engineering from Colorado State University, USA. He is currently a researcher in the Center for Energy and Environmental Sustainability, Prairie View A&M University. Dr. Du published over 10 journal papers and more than 20 presentations at regional, national and international conferences. His current research interests are carbon capture with polyamine functionalized nanomaterials, environmental sustainability and produced water treatment.

Riley H. Mullins is a senior student, a research assistant in the Department of Earth and Environmental Sciences at University of Northern Iowa, majoring in Environmental Science with an Air Quality minor. Over the past year she has worked with Dr. Xinhua Shen on various carbon capture with nanaomaterials and air quality related research projects. She will be graduating in May 2017 and then will be looking for a job as an Environmental Scientist.

Dr. Raghava R. Kommalapati received MS and PhD degrees in environmental engineering from Louisiana State University, LA, USA. Dr. Kommalapati is the Director of Center for Energy & Environmental Sustainability, a NSF funded center at Prairie View A&M University, Prairie view, TX, which is a part of the Texas A&M University System. He edited one book and published about 40 peer-reviewed journal articles and more than 90 proceedings and presentations at regional, national and international conferences. His research interests include remediation of contaminated soils, industrial waste separations, air quality atmospheric air-fog interactions and environmental impacts of energy technologies.

With the increasing availability of high performance computers, workstations and clusters, numerical computations have become popular in materials science and engineering. Highly parallelized computer systems today allow materials scientists to study material properties by solving complex, non-linear many body problems at different time and length scales with efficient algorithms[13] (shown as Figure 2). *Ab initio* calculations based on quantum mechanics using electron structure theory, i.e., density functional theory (DFT) with the Born-Oppenheimer approximation are performed at the time scale of femtosecond (fs) and picosecond (ps) and the length scales of Å and nm. Molecular dynamics (MD) and Monte Carlo (MC) simulations at the atomistic or microscopic scale, even mesoscale are used to investigate a wide range of properties from thermodynamics to bulk properties of solids and fluids at the time scales of nanosecond (ns), microsecond (µs) millisecond (ms) and second (s), and the length scales of nm, µm and mm. Computational fluid dynamics (CFD) simulations using continuum models perform the bulk calculations to investigate the interaction of gases, liquids, and moving particles with surfaces defined by boundary conditions at the greatest time and length scales. Amine-based adsorbents including MEA, amine oligomers and PEI have been theoretically studied from the electronic or atomic level with DFT to the grid level with CFD.

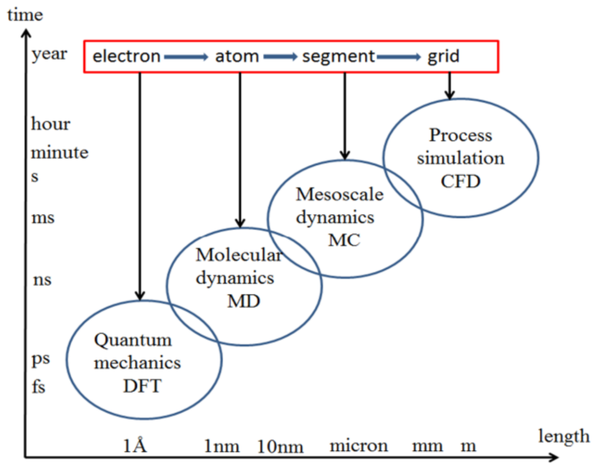

Figure 2. Computing techniques at different time and length scales.

2.1. Studied from DFT

DFT modeling uses the functional of the electron probability density, which is a function of space and time, to investigate the electronic structure of small atomic systems with the Born-Oppenheimer approximation[13]. Because solvent amines such as MEA and DEA have been used for CO_2 capture in the natural gas industry for a long time, the reactions between CO_2 and solvent amines were widely studied by using DFT modelling[14]. These studies help to understand the reaction mechanism of PEI with CO_2 due to the presence of primary and secondary amines in small amine molecules. The mechanisms of CO_2 reactions with MEA, DEA and ammonia to form carbamic acid and zwitterion pairs in the aqueous phase were investigated using DFT at the functionals of B3LYP and G3MP2B3 by Arstad et al.[14a], and the calculations using a solvent continuum model interpreted a large impact of surrounding water, MEA, DEA and ammonia species on activation and reaction energies. Gibbs free energies of MEA reactions with CO_2 in aqueous solution were calculated by using geometry optimizations in gas and aqueous phases with different basis sets, and the paper suggested that the B3LYP calculation with the dispersion correction significantly improved the results[14f]. With the B3LYP functional and 6-31+G(d,p) basis set, Lee et al. computed the energy and electronic structures of three classes of functionalized amines: alkylamines, alkanolamines, and fluorinated alkylamines along two main CO_2 capture pathways of bicarbonate and carbamate, and evaluated the reaction energies associated with the formation of amine-bicarbonate and amine-carbamate complexes in aqueous amine−CO_2 solution[15]. Zhao et al.[16] investigated the effect of chain length of low-molecular-weight PEI on physisorption and chemisorption of CO_2 using the reference interaction-site model (RISM) and DFT at the M06-2X/6-31G (d,p) level, and found that CO_2 capture capacities of both physisorption and chemisorption decrease as the chain length increases.

2.2. Studied from MD and MC

MD simulations are used to investigate the interactions of atoms and molecules based on classical intermolecular interaction potentials of covalent bonds, Coulomb interactions, torsion and bending in molecules and the Lennard-Jones potential between non-bonded atoms using the Newton's laws of motion[13]. MC molecular simulations rely on equilibrium statistical mechanics and employ a Markov chain procedure to determine a new state for a molecular system from a previous state[17]. The explicit or atomic models of MD and MC are used at the microscale, and the implicit models are used at the mesoscale where a cluster of atoms is considered a coarse grain, or the solvent is considered a continuous medium. Before the first modelling of CO_2 capture with PEI was performed with an MD or MC method, the protonation behaviors of linear PEI in solution have been investigated somewhere through MD and MC Simulations[18]. The partial atomic charges of PEI were determined by the RESP protocol using Gaussian 03 with the 6-31G* basis set, and the explicit modeling of a short linear PEI chain with 20 repeating units was carried out through MD simulation by using the Amber gaff force field. Later, PEI was modeled with a coarse-grained method where the parameters of grains were obtained from the first-step MD simulations. Two different functionalization methods, impregnation and grafting of PEI on MCM-41, were studied by using a grand canonical Monte Carlo (GCMC) method[19]. The comparison showed that the CO_2 adsorption capacity of impregnation is greater than grafting due to the mobility of the impregnated PEI chains. Wang et al. further investigated the interaction between PEI and MCM-41 in a solid adsorbent by optimizing the molecular system with MD simulations, and the CO_2 adsorption thermodynamics at various

PEI loadings through GCMC simulations[20]. Figure 3 shows the structures of PEI and MCM-41 before and after MD optimization in the study[20]. In addition to MCM-41 which owns an ordered structure, Builes et al. examined the CO_2 adsorption capacity of PEI functionalized on disordered silica gel SG40 using GCMC modeling[21].

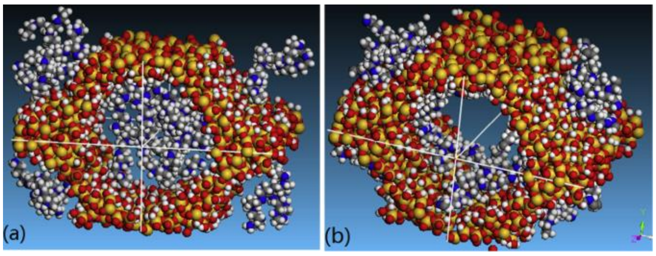

Figure 3. The structures of PEI/MCM-41 before (a) and after (b) optimization. (color code: yellow, Si; red, O; white H; blue, N; grey, C) (Adapted from Ref. 20).

2.3. Studied from CFD

CFD modeling is an engineering-based computational process to resolve different fluid flow related problems, including flow velocity, density, temperature, and concentration, and possesses some practical advantages, such as, foreseeing before installation, reliable results, cost and time savings. CFD modeling would help to accelerate the commercialization and deployment of PEI-based CO_2 capture technologies. Ryan et al.[22] carried out multi-phase CFD simulations of an amine-based solid sorbent carbon capture system by using two different Eulerian–Eulerian and Eulerian–Lagrangian models available in FLUENT® and BARRACUDA, and found that the Eulerian–Lagrangian model was the better option for modeling a solid amine adsorption system. Clark et al.[23] also used the Eulerian–Lagrangian model to simulate CO_2 capture in a full-loop circulating fluidized bed unit, and reached good results comparable to the experiments. The CFD study of the parametric behavior of solid-sorbent CO_2 absorption in a riser reactor[24] showed that the reactor performance would be improved by speeding up the cycling of the amine-functionalized solid particles in the reactor and reducing the gas flow. Figure 4a shows a typical cycling solid sorbent CO_2 capture system simulated by CFD modeling[24]. Another multi-phase CFD modeling was carried out to simulate a moving solid absorbent regenerator with a series of additional perforated plates along the regenerator height under plug flow and well mixed flow conditions, and CO_2 adsorption and desorption were performed[25]. Breault et al. compared the results of the 3-dimensional nonisothermal mult-phase CFD simulation using kinetics obtained from thermogravimetric analysis (TGA) with the batch experiments conducted by flowing mixed gases CO_2, N_2 and vapor through a fluidized bed, and found that the time duration of CO_2 capture decreased with the increase of gas flow[26]. Recently, Breault et al. further modified the amine-based solid sorbent CO_2 capture unit with the aid of CFD modeling, and an alternative 180 µm Geldart group B material was successfully used to replace the previous 115 µm Geldart group A material by keeping a constant circulation of a solid sorbent[27]. Figure 4b shows the 5 modifications (Mod 1, Mod 2, Mod 3, Mod 4 and Mod 5) of the carbon capture test unit following by the CFD simulations. The sequential modifications included the increase of the overall system height, the replacement of L-value, the height reduction of the riser, the volume extension of the regenerator, etc, which were described in detail in the ref[27]. The hydrodynamics and the reaction behavior in a fluidized bed reactor for solid sorbent CO_2 capture were also investigated by using CFD with integration of CO_2 adsorption kinetics, and the researchers concluded that the velocities of gas and solid particles were not uniform in the reactor and the CO_2 capture efficiency decreased with the increasing percentage of CO_2 in the feeding gas flow[28].

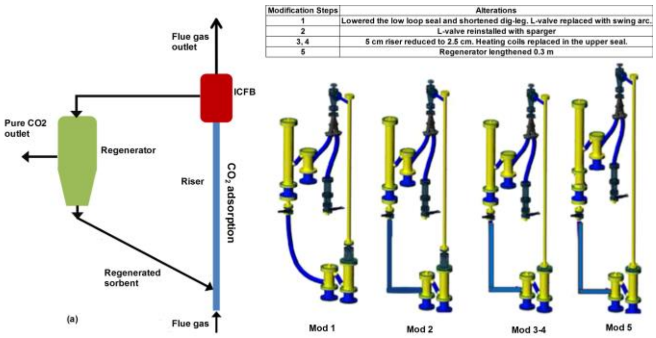

Figure 4. Typical solid sorbent CO_2 capture test system (a)[24] and the 5 modification steps for the amine-based solid sorbent CO_2 capture unit coupling with CFD modeling (b)[27] (Adapted from Ref. [24] and [27]).

3. Experimental Work

3.1. PEI Functionalized Silica

Since silica used as the support for a PEI-functionalized sorbent was first reported in the early 1990s where PEI was bonded to silica gel through a covalent bond[29], many kinds of silica materials such as MCM-41, SBA-15, SBA-16, KIT, etc.[7] have been explored to use as the support materials for amined-based adsorbents. Table 1 lists CO_2 capture by different PEI-functionalized silica materials under different conditions. Xu et al. first reported that a solid amine adsorbent was made from MCM-41 impregnated with PEI for carbon capture[30]. The CO_2 capture capacity depended on the CO_2 partial pressure and the presence of moisture, the highest was 133 mg/g at 1 atm[30b], and the lowest was 89 mg/g[30c]. The capacity (measured at 75°C) increased with the presence of moisture mainly due to the formation of carbamic acid, and the adsorbent could be regenerated at the same temperature. Later, the pore expanded MCM-41 was tested as the support by keeping the same pressure of 1 atm and the same adsorption temperature of 75°C, and much higher capacity of 210 mg/g was achieved because some long alkyl chains covered the pores to enhance the dispersion of PEI[31]. Inorganic alkali was also used to modify

MCM-41, and the capacity of 54 mg/g was reached at 50°C with the feeding simulated flue gas of 10% CO_2 and 90% N_2[32].

Table 1. CO_2 capture by different PEI-functionalized silica materials.

Support material	Branched/ linear PEI	CO_2 partial Pressure (atm)	Adsorption temp. (°C)	Equilibrium capacity (mg/g)		Regeneration temp. (°C)	Reference
				Dry condition	Humid condition		
MCM-41	Branched	0.005	75	48	-	75	[30a]
MCM-41	Branched	1	75	133	-	75	[30b]
MCM-41	Branched	0.15	75	89	131	75	[30c]
MCM-41	*	1	30	77	-	50	[33]
Pore expanded MCM-41	*	1	75	210	-	75	[31]
Pore expanded MCM-41	*	1	75	206	-	90, 100	[34]
Pore expanded MCM-41	Branched	1	45	96.9	-	45	[35]
Inorganic alkali modified MCM-41	*	0.1	50	54	-	100	[32]
MCM-48	*	0.24	80	94	-	140	[36]
MCM-48	Linear	1	75	119	-	75	[37]
SBA-15	Branched	1	45	88.2	-	45	[38]
SBA -15	Branched	1	75	173	-	85	[39]
SBA -15	Linear	0.15	75	105	-	100	[40]
SBA -15	Linear	0.15	75	140	-	110	[41]
SBA -15	Branched	0.15	45	55.6	86	110	[42]
SBA -15	Branched	1	0	77.9	-	100	[43]
SBA-15	Linear	1	75	127	-	75	[37]
SBA-15	Branched	0.15	45	71.2	-	110	[44]
SBA-15	Linear	0.15	75	140	-	100	[45]
Zr-SBA-15	*	0.0004	30	100		110	[46]
Pore expanded SBA -15	Branched	1	45	111.1	-	110	[47]
Pore expanded SBA -15	Branched	1	45	138		110	[48]
sulfonic-acid-functionalized SBA-15	*	0.07	75	-	100.9	105	[49]
SBA-16	linear	1	75	129	-	75	[37]
KIT-6	Linear	1	75	135	-	75	[37]
Mesocellular siliceous foam (MCF)	Branched	0.5	105	151	-	110	[50]
MCF	Linear	0.15	75	152	-	75	[51]
MCF	Branched	0.2	75	146	154	110	[52]
MCF	*	0.10	75	142.6	-	100	[53]
MCF	*	1	75	201	-	100	[54]
MCF	Branched	0.1	70	225	-	105	[55]
MCF	Branched	0.95	85	265	-	75	[56]
Mesoporous silica	Branched	0.15	70	95	106-110	130	[57]
Nano silica	Branched	1	105	186	-	120	[58]
Mesocellular siliceous foam with template	*	0.67	70	198	-	100	[59]
millimeter-sized spherical silica foams	Linear	1	75	188.3	-	100	[60]
Mesocellular silica	*	0.1	45	55	-	110	[61]
Mesocellular silica	Linear	1	75	218	-	75	[62]
HMS	Linear	1	75	184	-	75	[63]
Fumed silica	Branched	0.0004	25	52	78	85	[64]
K2CO3/fumed silica	*	0.15	75	120.9	120	120	[65]
G-silica sheet	*	7	75	190	-	120	[66]
CARiACT G10 silica	*	1	80	121	-	80	[67]

Silica monolith	Branched	1	75	210	260	75	[68]
Silica gel	*	5	35	44.4	-	35	[69]
Silica gel	*	0.15	75	138	185	100	[70]
Silica gel	Linear	0.151	75	93.4	-	100	[71]
Meso-macro porous silica	*	0.14	90	122	-	110	[72]
Mesoporous multilamellar silica vesicle	*	1	75	-	218	110	[73]
Mesoporous multilamellar silica vesicle	*	1	90	208	-	110	[73]

The symbol "*" means that the type (linear or branched) of PEI wasn't reported in the reference.

Sanz et al.[38] reported the CO_2 capture of SBA-15 impregnated with branched PEI (10, 30, 50 and 70 wt%) feeding with pure CO_2 and the corresponding capacities at 75°C under 1 bar were 25.2, 60.8, 75 and 88.2 mg/g. The capacity was also strongly influenced by temperature, and it was increased in the test range of 25–75°C. Heydari-Gorji et al.[39] compared the properties of calcined pore-expanded MCM-41, conventional SBA-15 and SBA-15 platelets with very short channels where all the supports were impregnated with PEI at the weight ratio of 50% and 55%, and reached the maximum capture capacity of 173 mg/g at the SBA-15 platelets in the environment of pure CO_2. They also found that the capacity increased in the temperature range of 25–75°C, and then decreased from 75°C in the range of 75–120°C. Another SBA-15 based adsorbent was also developed by the optimum combination of SBA-15 and linear PEI (M_w=423), and the sorption capacity of 140 mg/g was achieved by the presence of 15% CO_2 in the feeding gas[41].

Chen et al.[63] developed a series of hexagonal mesoporous silica (HMS) materials with different textural mesoporosities coated with PEI used as a CO_2 capture adsorbent, and found the textural mesoporosities played a very important role for loading PEI and facilitating CO_2 diffusion inside the pores. The maximum CO_2 capture capacity of 184mg/g was reached at 75°C with the PEI loading of 60 wt% in the pure CO_2 environment. Son et al.[37] compared a series of mesoporous silica materials, MCM-41, MCM-48, SBA-15, SBA-16, and KIT-6, used as the support materials for PEI-functionalized adsorbents, and reported that the CO_2 adsorption capacities of different adsorbents were in the order of KIT-6 ≈ SBA-16 > SBA-15 > MCM-48 > MCM-41. The KIT-6 with the largest pores exhibited the highest CO_2 adsorption capacity of 135 mg/g at 75°C with pure CO_2 feeding when PEI was loaded at the rate of 50 wt% of the support material. Yang et al.[66] synthesized sandwich-like graphene-based mesoporous silica (G-silica) sheets, in which graphene was confined between individual silica sheets with high surface areas, and compared the CO_2 adsorption capacities of PEI-impregnated G-silica sheets and PEI-impregnated silica sheets. A high adsorption capacity of 190 mg/g at the optimized temperature of 75°C was achieved with PEI-impregnated G-silica sheets because the interlayered graphene spacer was favorable for the efficient CO_2 diffusion and adsorption.

Ebner et al.[67] immobilized PEI into CARiACT G10 silica obtained from Fuji Silysia for a pressure swing CO_2 adsorption, and the study showed that the adsorbent was very stable under the conditions of the temperature from 40 to 100°C, the CO_2 partial ratio from 1.2 to 100 vol% with the total pressure fixed at 1 atm, and the relative humidity from dry conditions to 2 vol%. Subagyono et al.[50] developed a PEI-impregnated mesocellular siliceous foam (MCF) for CO_2 capture by loading linear PEI (M_w = 2500) or branched PEI (Mn = 1200). The adsorption capacity of MCF loaded with the branched PEI reached 151 mg/g at 105°C with 50 vol% CO_2 feeding, which was greater than the largest adsorption capacities of MCF loaded with the linear PEI (146 mg/g adsorbent) at 75°C and SBA-15 loaded with the branched PEI (107 mg/g adsorbent) at 105°C with the same feeding gas. Yan et al.[51] synthesized three MCF materials with different window sizes, which were used for the support materials of PEI-impregnated adsorbents, and the largest CO_2 capture capacity was reached by the PEI-impregnated FCM with largest window size at 75°C with the presence of 15.1 vol% CO_2 in the gas mixture of N_2 and CO_2. Zhang et al.[56] reported a hybrid PEI MCF used for CO_2 capture by loading PEI with different molecular weights (M_w=800, 1800, 25000), and the adsorption performance of the adsorbent impregnated with the PEI (M_w=25000) was very stable during 100 cyclic runs because of lower evaporation of PEI with higher M_w. A silica monolith with hierarchical mesomacroporous structures, large pore volume and textural mesoporosity was reported by Chen et al.[68], where the CO_2 adsorption capacity of 210 mg/g at 75°C was achieved with pure CO_2 feeding when PEI was loaded at the rate of 65 wt% of the support material. The adsorbent kept stable adsorption and regeneration performances during five repeated adsorption-desorption cycles and its adsorption capacity was much higher than those of the adsorbents made from other silica materials.

3.2. PEI Functionalized Nanotubes

Dillon et al.[74] first reported carbon nanotube based amine sorbents used for carbon capture, in which branched (M_w=600, 1800, 10000, and 25000 Da) or linear (M_w=25000 Da) PEI were attached to fluorinated single-wall carbon nanotubes (F-SWNTs) through direct convent bonding to the single walls. The characteristics of PEI-loaded F-SWNTs were examined through solid-state ^{13}C NMR, Raman spectroscopy, X-ray photoelectron spectroscopy, UV–vis spectroscopy, atomic force microscopy (AFM), and transmission electron microscopy (TEM), and the CO_2 adsorption capacity was investigated through TGA. The adsorption capacities of 41, 48, 52 and 72 mg/g were observed at 75°C under 1 atm for the F-SWNTs loaded with different branched PEIs (600, 1800, 10000 and 25000 D). The kinetics of CO_2 adsorption of PEI-functionalized SWNTs was compared to those of PEI-functionalized graphite oxide, and fullerene C60 using six different kinetic models: Elovich, pseudo-1st-order, pseudo-2nd-order, pseudo-nth-order, modified Avrami, and extended model[75]. The kinetics of CO_2 adsorption of PEI-functionalized SWNTs was observed to fit a pseudo-2nd-order model both under dry and humid conditions. Kong et al.[76] synthesized micro-nano carbonaceous composite activated carbon fiber/carbon nanotube (ACF/CNTs) used as the support material for a PEI-functionalized adsorbent, and the adsorption capacity of the adsorbent increased in the temperature range of 30-60°C, reached the maximum of 121.2 mg/g at 60°C, and then slightly decreased in the test range of 60-75°C. Lu's research group[77] first reported multi-wall carbon nanotubes (MWCNTs) used for CO_2 adsorption, in which the MWCNTs were modified by 3-aminopropyl-triethoxysilane (APTS) solution, and CO_2 adsorption was tested in the temperature range of 20-100°C. Lee et al.[78] synthesized PEI-impregnated MWCNTs through two steps: (1) pre-treatment of MWCNTs with HNO_3 and H_2SO_4, and (2) wet-impregnation of PEI, and the PEI-impregnated MWCNTs exhibited stable adsorption and desorption performance with the maximum CO_2 adsorption capacity of 15.5 mg/g at 40°C under flue gas conditions (15% CO_2/85% N_2). Liu et al.[79] investigated CO_2 adsorption of industrial grade multi-walled carbon nanotubes (IG-MWCNTs) functionalized with different branched PEIs (M_w=300, 600, 1800, 10000 and 70000), and the maximum CO_2 adsorption capacity of 111.7 mg/g was observed at 70°C with 10 vol% CO_2 present in the feeding gas (CO_2 and N_2) by keeping the constant gas flow rate of 50 cm^3/min, in which the CO_2 centration was monitored by gas chromatograph (GC). Lee[80] reported that silica-coated multi-walled carbon nanotubes, which were synthesized through the hydrolysis of tetraethylorthosilicate onto the surfaces of MWCNTs, were used as solid polyamine adsorbent after the impregnation of PEI with the molecular weight of 800. The adsorption behaviors of silica-coated MWCNTs impregnated at different PEI loading ratios of 10%, 20%, 30%, 40%, 50%, 60%, 70% and 80%, and the maximum of 28.5 mg/g was observed at 60°C under the flue gas condition (15 wt %CO_2/85 wt% N_2).

Table 2. CO_2 capture by different PEI-functionalized nanotubes.

Support material	Branched/ linear PEI	CO_2 partial Pressure (atm)	Temp. (°C)	Equilibrium capacity (mg/g)		Reference
				Dry condition	Humid condition	
Single-wall carbon nanotube	Branched	1	75	72	-	[74]
Activated carbon fiber/carbon nanotube composite	Branched	1	60	121.2	-	[76]
Multi-wall carbon nanotubes	Branched	0.15	40	15.3	-	[78]
Industrial multi-wall carbon nanotubes	Branched	0.1	70	111.7	-	[79]
Silica coated multi-wall carbon nanotubes	*	0.11	60	28.5	-	[80]
Halloysite nanotubes	*	0.0004	25	54.8	-	[81]
Halloysite nanotubes	Branched	1	75	61.6	-	[82]
Titanate nanotubes	*	1	75	129.4	-	[83]
Titanate nanotubes	Branched	0.1	75	134.6	-	[84]

The symbol "*" means that the type (linear or branched) of PEI wasn't reported in the reference.

Halloysite nanotubes(HNTs)[85], which is a kind of aluminosilicate clays, possess a hollow nanotubular structure with a diameter of about 20–50 nm and length of several hundred nm. Cai et al.[81] developed PEI-impregnated CO_2 adsorbents based on Halloysite nanotubes, which were characterized by Fouriertransform infrared spectrometry, gel permeation chromatography, dynamic light scattering, scanning electron microscopy (SEM), and TEM, the optimized capture capacity of 54.8 mg/g was obtained with 30% PEI loading, and the capture capacity kept reversible and stable during 50 cyclic adsorption–desorption runs. Kim et al.[82] compared two amine-functionalized HNTs: (3-aminopropyl) triethoxysilane(APTES)-grafted HNTs and PEI-impregnated HNTs, and found that the capture performance of (3-aminopropyl) triethoxysilane (APTES)-grafted HNTs was more advantageous over PEI-impregnated HNTs at a lower temperature of 50°C, while PEI-impregnated HNTs preferred to run at a higher temperature of 75°C.

Since the hydrothermal method was invented to fabricate TiO_2 based nanotubes[86], also called titanate nanotubes (TNTs), TNTs have intensively been studied for many applications, such as photocatalysis, electroluminescent hybrid devices, solar cells, batteries, etc[87]. Liu et al.[83] prepared protonated titanate nanotubes (PTNTs) in three steps: hydrothermal treatment from TiO2 powder, 0.1 M HCl washing the product obtained in the first step to the pH value of 1.6, and then deionized water washing to neutral. The obtained product was denoted as PTNTs and impregnated with PEI. The CO_2 capture capacity of PEI-impregnated PTNTs was determined via TGA, and it reached 129.4 mg/g at 75°C with the pure CO_2 feeding. Later, Guo et al.[84] compared the CO_2 capture capacity of PEI-impregnated PTNTs with that of triethylenetetramine(TETA)-impregnated PTNTs, where PTNTs were made from anatase TiO_2 powder. The maximum capture capacity of PEI-impregnated PTNTs of 134.6 mg/g was obtained with 50 wt% PEI loading, however, it was lower than that of TETA-impregnated PTNTs which were optimized with 60 wt% TETA loading. Both PEI-impregnated PTNTs displayed good stability and regeneration ability during the adsorption and desorption cycles feeding with simulated flue gas. Table 2 lists CO_2 capture by different PEI-functionalized nanotubes under different conditions.

3.3 PEI functionalized Membranes

Some gas mixtures can be effectively separated with membrane technologies, and commonly used membranes are generally made from polyamide, cellulose acetate, or ceramic materials. However, it is difficult to separate CO_2 and N_2 with general membranes because the molecular sizes of CO_2 and N_2 are very close. When PEI is incorporated into membranes for CO_2 separation, PEI can act as CO_2 carrier since its amine groups can react with CO_2 to form carbamate. Matsuyama et al.[88] developed a facilitated transport membrane from the blend of PEI and poly(vinyl alcohol)(PVA), and the CO_2/N_2 selectivity of over 230 by using the membrane was achieved at 25°C with the CO_2 partial pressure of 0.065 atm. A fixed carrier facilitated transport membrane for CO_2 separation[12] was prepared by coating a thin blending layer of PEI-PVA onto a polyethersulphone(PES) hollow fiber membrane, and a CO_2/N_2 selectivity reached up to 300 at 1 bar. Shen et al.[89] cast PEI and carboxymethyl chitosan onto polysulfone (PSF) ultrafiltration membranes, and the optimized membrane with 30 wt% PEI loading has the permeance of 630 GPU for CO_2 gas and a CO_2/N_2 selectivity of 325 at 2 atm. Mondal et al.[90] developed thermally stable crosslinked thin film composite PVA/polyvinylpyrrolidone(PVP) blend membranes doped with PEI for CO_2 separation, and the maximum CO_2/N_2 selectivity of 270 and a CO_2 permeance of 29 GPU were achieved at 100°C with optimization of membrane design. Liao et al.[91] copolymerized PEI with epichlorohydrin, and the resultant product (PEIE) could act as a raw material to build up hydrotalcite (HT), which is known as a layered double hydroxide, because the product has much higher molecular weight and more hydroxyl groups with grafting reactivity. The PEIE-HT was cast onto a porous polysulfone ultrafiltration membrane to fabricate a high-speed facilitated transport membrane. Figure 5 shows schematic CO_2 transport mechanism through the fixed carrier and high-speed facilitated transport membranes. The CO_2 permeance of 5693 GPU was achieved with the CO_2/N_2 selectivity of 268 at the feeding pressure of 0.11 MPa.

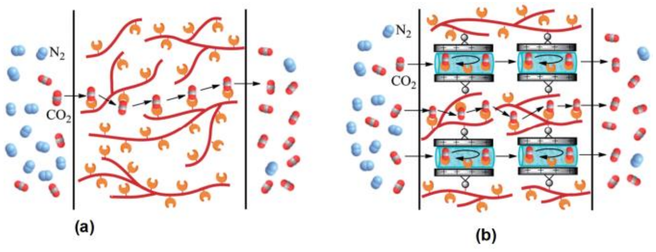

Figure 5: Schematic CO_2 transport mechanism through fixed carrier (a) and high-speed (b) facilitated transport membranes (Adapted from Ref. 91).

Recently, some PEI functionalized mixed matrix membranes were developed for CO_2 separation because of their significant improvement in separation properties with trivial loss in membrane flexibility compared to conventional polymeric membranes[92]. Wu et al.[92a] successfully incorporated PEI-functionalized mesoporous silica (PEI-MCM-41) into poly(ether-block-amide) to fabricate facilitated transport mixed matrix. The incorporated PEI distributed in MCM-41 pores and on MCM-41 surfaces not only facilitated the transport of CO_2 through reversible reaction, but also strengthened the rigidity of polymer chains at the filler–polymer interfaces, thus improving gas permeability and selectivity. Alternative SiO_2 nanoparticles functionalized with PEI[92g] were recently used to incorporate into cross-linked polyethylene glycol(PEG)-based polymer, and the resultant ultra-thin film composite mixed matrix membranes enhanced the CO_2 permeance up to 1300 GPU with a CO_2/N_2 selectivity of 27. Similarly, Xin et al. developed sulfonated poly(etheretherketone) (SPEEK)/PEI-functionalized TiO_2 submicrospheres mixed matrix membranes by using dopamine and PEI, and the optimized selectivities of the membranes for CO_2/CH_4 and CO_2/N_2 were 58 and 64[92b]. Further, Xin et al. enhanced the optimized selectivities to 71.8 for CO_2/CH_4 and to 80 for CO_2/N_2 by incorporating PEI-modified metal−organic frameworks into SPEEK[92f]. PEI-functionalized graphene oxide nanosheets used as fillers[92c] were incorporated into a commercial low-cost pristine Pebax membrane, and the optimized membrane with 10 wt% PEG-PEI- graphene oxide displayed a CO_2/CH_4 selectivity of 45, and a CO_2/N_2 selectivity of 120. Shen et al.[92e] grafted hyperbranched PEI onto graphene oxide nanosheets (HPEI-GO), and further cast HPEI-GO and chitosan onto a porous polysulfone support. The resultant mixed matrix membrane reached a CO_2/N_2 selectivity of 107 with 3.0 wt% HPEI-GO coating. Dong et al.[92h] also applied hyperbranched PEI and graphene oxide nanosheets onto a polysulfone support to prepare a fixed carrier composite membrane by incorporating trimesoyl chloride(TMC). The produced membrane displayed the highest CO_2 permeance of 9.7 GPU and the CO_2/N_2 selectivity of over 80 when it was tested with CO2/N2 (10:90 v:v) gas mixture.

3.4 PEI Functionalized Other Materials

In addition to different silica materials, carbon or titanate nanotubes and membranes, many researchers loaded PEI onto or directly synthesized into other various materials, such as, mesoporous alumina[93], bentonite[94], clay[95], activated carbon[96], fly ash[97], layered silicate[98], mesoporous carbon[99], mesoporous sponge-like TUD-1[100], metal organic frameworks (MOF)[101], nanofibrillated cellulose[102], porous chitosan beads[103], resin[104], glass fiber[105], polypropylene fiber[106], polyamide imide hollow fiber[107], ZSM-5 zeolite[108], ZIF-8[109], etc.. The CO_2 capture performances of other materials functionalized with PEI are demonstrated in Table 3. Chaikittisilp et al.[93b] compared PEI-impregnated mesoporous γ-alumina with some SBA-15-supported PEI adsorbents and concluded that the PEI-impregnated mesoporous γ-alumina is better on both capture capacity and amine efficiency, especially at ambient air conditions. The low-cost activated carbon, mesoporous carbons and glass fibers were used as the support materials by several research groups[96, 99, 105]. Wang et al.[99] tested the CO_2 capture capacities and stability of PEI-impregnated mesoporous carbons under different conditions of 15% CO_2, low concentration CO_2, ambient air, high temperature, temperature low to 0°C, and with or without the presence of moisture, and the results displayed the excellent CO_2 capture performance and great stability.

3.5 CO_2 capture with PEI from flue gas or air

CO_2 contributions from power plants account for about one third of total CO_2 emissions in the world. The flue gas emitted from coal, gas or oil based power plants contains 12-18% CO_2 with more than 66% N_2, some vapor and small percentages of nitrogen oxides and sulfur oxides. In order to prevent the irreversible reactions of nitrogen oxides and sulfur oxides with PEI, nitrogen oxides need to be treated by optimized modification of burning process or catalytic reactions with ammonia or urea, and sulfur oxides need to be removed by gas flue-gas desulfurization before CO_2 capture with PEI. In most lab-scaled experiments the flue gas was replaced with simulated flue gas, i.e., gas mixture of N_2, CO_2 with or without the presence of moisture and/or O_2. PEI-functionalized MCM-41[30c], SBA-15[42], mesocellular siliceous foam[51], silica gel[70], carbon nanotubes[78], titinate nanotubes[83], mesoporous carbon[99a], etc. have been tested feeding with simulated flue gas. The CO_2 capture capacities of PEI solid adsorbents are commonly lower than those under higher partial pressure of CO_2 or pure CO_2 conditions, and the presence of moisture enhances the CO_2 capture capacities of PEI solid adsorbents because the water molecule acts as a proton transfer agent in the reaction of CO_2 and amine groups. For example, Sanz-Perez et al.[42] prepared amine-functionalized SBA-15 through impregnation or grafting of PEI and TEPA, and found that SBA-15 impregnated with branched PEI enhanced the adsorption capacity around 55% with the presence of 5 wt% moisture.

Table 3. CO_2 capture by different PEI-functionalized other materials

Support material	Branched/ linear PEI	CO_2 partial Pressure (atm)	Temp. (°C)	Equilibrium capacity (mg/g)		Reference
				Dry condition	Humid condition	
Mesoporous alumina	Linear	1	75	120	-	[93a]
Mesoporous γ-alumina	branched	0.0004	25	77	-	[93b]
Bentonite	Linear	1	75	47	-	[94]
Clay (nanosized)	*	0.1	85	65	-	[95]
Commercial activated carbon	*	1	25	49	-	[96a]
K_2CO_3/ activated carbon	*	0.08	60	52.8	158	[96b]
Fly ash	*	0.1	90	145		[97]
Layered silicate	Branched	0.05	75	268.8	-	[98]
Mesoporous carbon	*	0.15	75	212	235.8	[99a]
Mesoporous carbon	Branched	0.0004	25	99	113.5	[99b]
Mesoporous carbon	Branched	1	0	123	-	[99c]
Mesoporous carbon	Branched	1	30	205	-	[99c]
Mesoporous sponge-like TUD-1	*	0.15	75	116	130	[100]
MOF	Linear	1	50	198	-	[101]
Nanofibrillated cellulose	Branched	0.0004	25	97	-	[102]
Porous chitosan bead	*	0.15	40	101	158	[103]
Resin	*	0.0004	25	99.3	-	[104a]
Resin	*	1	25	181	-	[104a]
Resin	*	1	25	178		[104b]
Glass fiber	Branched	0.24	30	182.6	-	[105]
Polypropylene fiber	Branched	0.1	25	-	260	[106a]
Polypropylene fiber	Branched	0.1	30	235.4	-	[106b]
Polyamide imide hollow fiber	Branched	0.01	35	48.4	61.6	[107]
ZSM-5 zeolite	Branched	1	40	116	-	[108]
ZIF-8	*	0.5	65	70.8	87.6	[109]

The symbol "*" means that the type (linear or branched) of PEI wasn't reported in the reference.

Relative to CO_2 capture from flue gas, CO_2 capture from air is more difficult because the even lower CO_2 concentration of 400 ppm in air. PEI-functionalized Zr-doped SBA-15[46], fumed silica[64], Halloysite nanotubes[81], mesoporous carbon[99b], nanofibrillated cellulose[102], facilitated transport membrane[12], etc. have been tested to capture CO_2 from air. For example, Goeppert et al.[64] reported that fumed silica impregnated with 33 wt% branched PEI (M_w=25000) possessed the stable CO_2 capture capacities of 52 mg/g under dry air condition and 78 mg/g under humid air condition at 25°C. The presence of moisture also enhances the CO_2 capture capacities of PEI solid adsorbents under ambient condition.

Compared to the absorbent regeneration in CO_2 capture with the MEA solution, the regeneration of PEI-functionalized solid adsorbents requires lower pressure and less energy[110]. The temperatures for the adsorbent recovery can be equal or higher than the adsorption temperatures during CO_2 capture from flue gas[30a, 40, 51, 83]. For the case of CO_2 capture from air, the desorption temperature is usually set up in a mild or high range of 70-130°C to speed up CO_2 release[64, 111]. In a CO_2 capture scenario with a capture capacity of 40 ton-CO_2/day described by Zhang et al.[111b], a total thermal energy of 3.2 GJ/ton-CO_2 was required for the whole cycle of adsorption and desorption, and the regeneration thermal heat was estimated to 3.2 GJ/ton-CO_2.

4. Conclusions

In order to overcome the drawbacks of solvent amines such as, MEA and DEA, scientists and engineers are looking for some great alternatives for CO_2 capture. Different PEIs have widely been investigated to functionalize different solid support materials used for CO_2 capture in recent 15 years. This review article provides an overview of the recent advances of such PEI-functionalized adsorbents, in which PEI are loaded on different silica materials, nanotubes, membranes and other materials such as, mesoporous alumina, clay, activated carbon, fly ash, mesoporous carbon, mesoporous sponge-like TUD-1, metal organic frameworks, nanofibrillated cellulose, porous chitosan bead, resin, glass fiber, zeolites, etc..

The limited *ab initio* calculations showed that CO_2 capture capacities of the PEI-functionalized adsorbents decreased with the increase of the chain length for the low-molecular-weight PEI; molecular dynamics and Monte Carlo simulations of different amine-based sorbents discovered the interactions of PEI with the support materials, and the enhancement of water on CO_2 capture. Computational fluid dynamics simulations of solid amine adsorbents helped on the commercialization and deployment of PEI-based CO_2 capture technologies in some pilot applications at the industrial level. Mesoporous silica materials are the most widely investigated materials used as the supports of PEI-functionalized adsorbents because of their availability and various nanosized pores. Some PEI-functionalized silica adsorbents via impregnation of PEI displayed large CO_2 capture capacity and excellent stability up to 50 or 100 cyclic runs of adsorption and desorption of CO_2. In addition, the presence of moisture enhances the CO_2 capture capacity for both conditions of flue gas and the ambient environment. Some PEI-functionalized nanotubes, mesoporous alumina, mesoporous carbons, etc.. displayed similar CO_2 capture performances to those of PEI-functionalized mesoporous silica materials. The CO_2 capture performance of some PEI-impregnated mesoporous carbons proved that carbon can be a strong candidate for polyamine-loading because of its abundance, low cost and surface functionality. The applications of PEI in some facilitated transported membranes enhanced the selectivity and permeance of CO_2 because PEI chains in the membranes work as CO_2 carriers.

Acknowledgements

This work is partially supported by a grant from the Department of Energy, National Energy Technology Laboratory Grant DE-FE0023040; National Science Foundation (NSF) through the Center for Energy and Environmental Sustainability (CEES), a NSF CREST Center, Award #1036593; and University of Northern Iowa faculty 2016 summer fellowship.

Keywords: CO_2 capture • polyethylenimine • silica • nanotube • membrane

[1] a) J. Burger, J. Clarke, M. Gochfeld, *Environ. Monit. Assess.* **2011**, *172*, 121-134; b) R. E. Kasperson, B. J. Ram, *Daedalus* **2013**, *142*, 90-96; c) X. Shen, R. R. Kommalapati, Z. Huque, *Sustainability* **2015**, *7*, 12974-12987.
[2] a) M. Wang, A. Lawal, P. Stephenson, J. Sidders, C. Ramshaw, *Chem. Eng. Res. Des.* **2011**, *89*, 1609-1624; b) M. Wang, A. S. Joel, C. Ramshaw, D. Eimer, N. M. Musa, *Appl.Energy* **2015**, *158*, 275-291; c) B. Sreenivasulu, D. V. Gayatri, I. Sreedhar, K. V. Raghavan, *Renew. Sust. Energ. Rev.* **2015**, *41*, 1324-1350.
[3] a) S. Fogarasi, C.-C. Cormos, *J. Clean Prod.* **2015**, *103*, 140-148; b) D. P. Hanak, C. Biliyok, V. Manovic, *Inter. J. Greenh. Gas Con.* **2015**, *34*, 52-62; c) Z. Zhang, *Energy Environ.* **2015**, *26*, 1069-1080.
[4] M. K. Mondal, H. K. Balsora, P. Varshney, *Energy* **2012**, *46*, 431-441.
[5] a) H. Q. Yang, Z. H. Xu, M. H. Fan, R. Gupta, R. B. Slimane, A. E. Bland, I. Wright, *J,Environ,Sci.* **2008**, *20*, 14-27; b) S. Rafiq, L. Y. Deng, M. B. Hagg, *Chembioeng Rev.* **2016**, *3*, 68-85.
[6] B. P. Spigarelli, S. K. Kawatra, *J. CO₂ Util.* **2013**, *1*, 69-87.
[7] C. Chen, J. Kim, W. S. Ahn, *Korean J. Chem. Eng.* **2014**, *31*, 1919-1934.
[8] a) D. M. D'Alessandro, B. Smit, J. R. Long, *Angew. Chem. Int. Ed.* **2010**, *49*, 6058-6082. b) D. D. Miller, S. S. C. Chuang, *J. Phys. Chem. C* **2016**, *120*, 25489-25504; c) J. Yu, S. S. C. Chuang, *Energy Fuels* **2016**, *30*, 7579-7587; d) S. A. Didas, M. A. Salcwa-Novak, G. S. Foo, C. Sievers, C. W. Jones, *J. Phys. Chem. Lett.* **2014**, *5*, 4194-4200.
[9] a) Z. A. Chen, M. C. Deng, C. Yong, G. H. He, W. Ming, J. D. Wang, *J. Membrane Sci.* **2004**, *235*, 73-86; b) L. Wagberg, *Nordic Nord Pulp Pap. Res. J.* **2000**, *15*, 586-597.
[10] S. Satyapal, T. Filburn, J. Trela, J. Strange, *Energy Fuels* **2001**, *15*, 250-255.
[11] Q. A. Wang, J. Z. Luo, Z. Y. Zhong, A. Borgna, *Energy. Environ.Sci.* **2011**, *4*, 42-55.
[12] M. S. Abd Rahaman, L. Zhang, L. H. Cheng, X. H. Xu, H. L. Chen, *Rsc Adv.* **2012**, *2*, 9165-9172.
[13] M. O. Steinhauser, S. Hiermaier, *Int. J. Mol. Sci.* **2009**, *10*, 5135-5216.
[14] a) B. Arstad, R. Blom, O. Swang, *J. Phys. Chem. A* **2007**, *111*, 1222-1228; bA. Maiti, W. L. Bourcier, R. D. Aines, *Chem. Phys. Lett.* **2011**, *509*, 25-28; c) H. Yamada, Y. Matsuzaki, T. Higashii, S. Kazama, *J. Phys. Chem. A* **2011**, *115*, 3079-3086; d) T. Davran-Candan, *J. Phys. Chem. A* **2014**, *118*, 4582-4590; e) S. A. Didas, R. S. Zhu, N. A. Brunelli, D. S. Sholl, C. W. Jones, *J. Phys. Chem. C* **2014**, *118*, 12302-12311; f) S. Y. Lee, *B. Korean Chem. Soc.* **2015**, *36*, 2795-2796; g) P. Jackson, *Struct. Chem.* **2014**, *25*, 1535-1546; h) B. Han, C. G. Zhou, J. P. Wu, D. J. Tempel, H. S. Cheng, *J. Phys. Chem. Lett.* **2011**, *2*, 522-526.
[15] A. S. Lee, J. R. Kitchin, *Ind. Eng. Chem. Res.* **2012**, *51*, 13609-13618.
[16] Q. Zhao, Q. Wang, C. Zhang, Z. Du, M. Tian, J. Mi, *Chemphyschem* **2015**, *16*, 1480-1490.
[17] Z. Q. Tian, S. Dai, D. E. Jiang, *Wiley Interdiscip. Rev. Comput. Mol. Sci.* **2016**, *6*, 173-197.
[18] J. D. Ziebarth, Y. M. Wang, *Biomacromolecules* **2010**, *11*, 29-38.
[19] S. Builes, L. F. Vega, *Langmuir* **2013**, *29*, 199-206.
[20] W. L. Wang, J. Li, X. L. Wei, J. Ding, H. J. Feng, J. Y. Yan, J. P. Yang, *Appl. Energy* **2015**, *142*, 221-228.
[21] S. Builes, P. Lopez-Aranguren, J. Fraile, L. F. Vega, C. Domingo, *Energy Fuels* **2015**, *29*, 3855-3862.

[22] E. M. Ryan, D. DeCroix, R. Breault, W. Xu, E. D. Huckaby, K. Saha, S. Dartevelle, X. Sun, *Powder Technol.* **2013**, *242*, 117-134.

[23] S. Clark, D. M. Snider, J. Spenik, *Powder Technol.* **2013**, *242*, 100-107.

[24] R. W. Breault, E. D. Huckaby, *Appl. Energy* **2013**, *112*, 224-234.

[25] A. Sarkar, W. X. Pan, D. Suh, E. D. Huckaby, X. Sun, *Powder Technol.* **2014**, *265*, 35-46.

[26] R. W. Breault, L. J. Shadle, J. L. Spenik, E. D. Huckaby, *J.Comput, Environ. Sci.* **2014**, *2014*, 14.

[27] R. W. Breault, J. L. Spenik, L. J. Shadle, J. S. Hoffman, M. L. Gray, R. Panday, R. C. Stehle, *Chem. Eng. Res. Des.* **2016**, *112*, 251-262.

[28] J. Chang, K. Zhang, Y. P. Yang, B. D. Wang, Q. Sun, *Powder Technol.* **2015**, *275*, 94-104.

[29] T. Tsuda, T. Fujiwara, *J. Chem. Soc., Chem. Commun.* **1992**, 1659-1661.

[30] a) X. C. Xu, C. S. Song, J. M. Andresen, B. G. Miller, A. W. Scaroni, *Energy Fuels* **2002**, *16*, 1463-1469; b) X. C. Xu, C. S. Song, J. M. Andresen, B. G. Miller, A. W. Scaroni, *Micropor. Mesopor. Mat.* **2003**, *62*, 29-45; c) X. C. Xu, C. S. Song, B. G. Miller, A. W. Scaroni, *Ind. Eng. Chem. Res.* **2005**, *44*, 8113-8119.

[31] A. Heydari-Gorji, Y. Belmabkhout, A. Sayari, *Langmuir* **2011**, *27*, 12411-12416.

[32] Y. Teng, L. J. Li, G. Xu, K. Zhang, K. X. Li, *Energies* **2016**, *9*.

[33] H. Kassab, M. Maksoud, S. Aguado, M. Pera-Titus, B. Albela, L. Bonneviot, *Rsc Adv.* **2012**, *2*, 2508-2516.

[34] A. Heydari-Gorji, A. Sayari, *Chem. Eng. J.* **2011**, *173*, 72-79.

[35] R. Sanz, G. Calleja, A. Arencibia, E. S. Sanz-Perez, *Micropor. Mesopor. Mat.* **2015**, *209*, 165-171.

[36] P. Sharma, J. K. Seong, Y. H. Jung, S. H. Choi, S. D. Park, Y. Il Yoon, I. H. Baek, *Powder Technol.* **2012**, *219*, 86-98.

[37] W. J. Son, J. S. Choi, W. S. Ahn, *Micropor. Mesopor. Mat.* **2008**, *113*, 31-40.

[38] R. Sanz, G. Calleja, A. Arencibia, E. S. Sanz-Perez, *Appl. Surf. Sci.* **2010**, *256*, 5323-5328.

[39] A. Heydari-Gorji, Y. Yang, A. Sayari, *Energy Fuels* **2011**, *25*, 4206-4210.

[40] X. L. Yan, L. Zhang, Y. Zhang, G. D. Yang, Z. F. Yan, *Ind. Eng. Chem. Res.* **2011**, *50*, 3220-3226.

[41] X. L. Ma, X. X. Wang, C. S. Song, *J. Am. Chem. Soc.* **2009**, *131*, 5777-5783.

[42] E. S. Sanz-Perez, M. Olivares-Marin, A. Arencibia, R. Sanz, G. Calleja, M. M. Maroto-Valer, *Inter. J. Greenh. Gas Con.* **2013**, *17*, 366-375.

[43] X. Yan, S. Komarneni, Z. Yan, *J. Colloid Interface Sci.* **2013**, *390*, 217-224.

[44] R. Sanz, G. Calleja, A. Arencibia, E. S. Sanz-Perez, *Micropor. Mesopor. Mat.* **2012**, *158*, 309-317.

[45] X. X. Wang, X. L. Ma, C. S. Song, D. R. Locke, S. Siefert, R. E. Winans, J. Mollmer, M. Lange, A. Moller, R. Glaser, *Micropor. Mesopor. Mat.* **2013**, *169*, 103-111.

[46] M. A. Sakwa-Novak, A. Holewinski, C. B. Hoyt, C. J. Yoo, S. H. Chai, S. Dai, C. W. Jones, *Langmuir* **2015**, *31*, 9356-9365.

[47] R. Sanz, G. Calleja, A. Arencibia, E. S. Sanz-Perez, *Energy Fuels* **2013**, *27*, 7637-7644.

[48] A. Olea, E. S. Sanz-Perez, A. Arencibia, R. Sanz, G. Calleja, *Adsorption* **2013**, *19*, 589-600.

[49] J. Liu, D. D. Cheng, Y. Liu, Z. B. Wu, *Energy Fuels* **2013**, *27*, 5416-5422.

[50] D. J. N. Subagyono, Z. Liang, G. P. Knowles, A. L. Chaffee, *Chem. Eng. Res. Des.* **2011**, *89*, 1647-1657.

[51] X. Yan, L. Zhang, Y. Zhang, K. Qiao, Z. Yan, S. Komarneni, *Chem. Eng. J.* **2011**, *168*, 918-924.

[52] D. J. N. Subagyono, M. Marshall, G. P. Knowles, A. L. Chaffee, *Micropor. Mesopor. Mat.* **2014**, *186*, 84-93.

[53] J. J. Ma, Q. M. Liu, D. D. Chen, Y. Zhou, S. Wen, *J. Mater.Sci.* **2014**, *49*, 7585-7596.

[54] W. Wang, X. Wang, X. Ma, E. Fillerup, C. Song, *Catal. Today* **2014**, *233*, 100-107.

[55] Z. Y. Liu, D. Pudasainee, Q. X. Liu, R. Gupta, *Sep. Purif. Technol* **2015**, *156*, 259-268.

[56] H. Zhang, A. Goeppert, M. Czaun, G. K. S. Prakash, G. A. Olah, *Rsc Adv.* **2014**, *4*, 19403-19417.

[57] W. B. Zhang, H. Liu, C. Sun, T. C. Drage, C. E. Snape, *Chem. Eng. J.* **2014**, *251*, 293-303.

[58] K. Li, J. Jiang, S. Tian, F. Yan, X. Chen, *Journal of Materials Chemistry A* **2015**, *3*, 2166-2175.

[59] W. Yan, J. Tang, Z. J. Bian, J. Hu, H. L. Liu, *Ind. Eng. Chem. Res.* **2012**, *51*, 3653-3662.

[60] Y. Han, G. Hwang, H. Kim, B. Z. Haznedaroglu, B. Lee, *Chem. Eng. J.* **2015**, *259*, 653-662.

[61] W. Li, P. Bollini, S. A. Didas, S. Choi, J. H. Drese, C. W. Jones, *ACS Appl. Mater. Interfaces* **2010**, *2*, 3363-3372.

[62] J.-E. Park, H.-K. Youn, S.-T. Yang, W.-S. Ahn, *Catal. Today* **2012**, *190*, 15-22.

[63] C. Chen, W. J. Son, K. S. You, J. W. Ahn, W. S. Ahn, *Chem. Eng. J.* **2010**, *161*, 46-52.

[64] A. Goeppert, M. Czaun, R. B. May, G. K. S. Prakash, G. A. Olah, S. R. Narayanan, *J. Am. Chem. Soc.* **2011**, *133*, 20164-20167.

[65] X. X. Wang, C. S. Song, *Energy Fuels* **2014**, *28*, 7742-7745.

[66] S. B. Yang, L. Zhan, X. Y. Xu, Y. L. Wang, L. C. Ling, X. L. Feng, *Adv. Mater.* **2013**, *25*, 2130-2134.

[67] A. D. Ebner, M. L. Gray, N. G. Chisholm, Q. T. Black, D. D. Mumford, M. A. Nicholson, J. A. Ritter, *Ind. Eng. Chem. Res.* **2011**, *50*, 5634-5641.

[68] C. Chen, S. T. Yang, W. S. Ahn, R. Ryoo, *Chem. Commun.* **2009**, 3627-3629.

[69] T. Zhu, S. Yang, D. K. Choi, K. H. Row, *Korean J. Chem.Eng.* **2010**, *27*, 1910-1915.

[70] Z. H. Zhang, X. L. Ma, D. X. Wang, C. S. Song, Y. G. Wang, AlChE J. **2012**, *58*, 2495-2502.

[71] K. Wang, H. Shang, L. Li, X. Yan, Z. Yan, C. Liu, Q. Zha, *J. Nat. Gas Chem.* **2012**, *21*, 319-323.

[72] T. Witoon, *Mater. Chem. Phys.* **2012**, *137*, 235-245.

[73] L. H. Zhang, N. Zhan, Q. Jin, H. L. Liu, J. Hu, *Ind. Eng. Chem. Res.* **2016**, *55*, 5885-5891.

[74] E. P. Dillon, C. A. Crouse, A. R. Barron, *ACS Nano* **2008**, *2*, 156-164.

[75] E. Andreoli, L. Cullum, A. R. Barron, *Ind. Eng. Chem. Res.* **2015**, *54*, 878-889.

[76] Y. X. Kong, L. Jin, J. Qiu, *Sci. Total Environ.* **2013**, *463*, 192-198.

[77] a) F. S. Su, C. S. Lu, W. F. Cnen, H. L. Bai, J. F. Hwang, *Sci. Total Environ.* **2009**, *407*, 3017-3023; b) S. C. Hsu, C. S. Lu, F. S. Su, W. T. Zeng, W. F. Chen, *Chem. Eng. Sci.* **2010**, *65*, 1354-1361.

[78] M.-S. Lee, S.-Y. Lee, S.-J. Park, *Int. J. Hydrogen Energy* **2015**, *40*, 3415-3421.

[79] Q. Liu, Y. Shi, S. Zheng, L. Ning, Q. Ye, M. Tao, Y. He, *J. Energy Chem.* **2014**, *23*, 111-118.

[80] M. S. Lee, S. J. Park, *J. Solid State Chem.* **2015**, *226*, 17-23.

[81] H. Cai, F. Bao, J. Gao, T. Chen, S. Wang, R. Ma, *Environ. Technol.* **2015**, *36*, 1273-1280.

[82] J. Kim, I. Rubino, J. Y. Lee, H. J. Choi, *Mater. Res. Express* **2016**, *3*.

[83] J. Liu, Y. Liu, Z. Wu, X. Chen, H. Wang, X. Weng, *J. Colloid Interface Sci.* **2012**, *386*, 392-397.

[84] L. P. Guo, J. Yang, G. S. Hu, X. Hu, H. DaCosta, M. H. Fan, *Nano Energy* **2016**, *25*, 1-8.

[85] M. L. Du, B. C. Guo, D. M. Jia, *Polym. Int.* **2010**, *59*, 574-582.

[86] T. Kasuga, M. Hiramatsu, A. Hoson, T. Sekino, K. Niihara, *Langmuir* **1998**, *14*, 3160-3163.

[87] H. H. Ou, S. L. Lo, *Sep. Purif. Technol* **2007**, *58*, 179-191.

[88] H. Matsuyama, A. Terada, T. Nakagawara, Y. Kitamura, M. Teramoto, *J. Membrane Sci.* **1999**, *163*, 221-227.

[89] J. N. Shen, C. C. Yu, G. N. Zeng, B. van der Bruggen, *Int. J. Mol. Sci.* **2013**, *14*, 3621-3638.

[90] A. Mondal, B. Mandal, *J. Membrane Sci.* **2014**, *460*, 126-138.
[91] J. Y. Liao, Z. Wang, C. Y. Gao, S. C. Li, Z. H. Qiao, M. Wang, S. Zhao, X. M. Xie, J. X. Wang, S. C. Wang, *Chem. Sci.* **2014**, *5*, 2843-2849.
[92] a) H. Wu, X. Q. Li, Y. F. Li, S. F. Wang, R. L. Guo, Z. Y. Jiang, C. Wu, Q. P. Xin, X. Lu, *J. Membrane Sci.* **2014**, *465*, 78-90; b) Q. P. Xin, H. Wu, Z. Y. Jiang, Y. F. Li, S. F. Wang, Q. Li, X. Q. Li, X. Lu, X. Z. Cao, J. Yang, *J. Membrane Sci.* **2014**, *467*, 23-35; c) X. Li, Y. Cheng, H. Zhang, S. Wang, Z. Jiang, R. Guo, H. Wu, *ACS Appl. Mater. Interfaces* **2015**, *7*, 5528-5537; d) E. M. Eminoglu, F. Beypinar, M. V. Kahraman, A. Durmus, *Polymer. Adv. Tech.* **2015**, *26*, 1053-1058; e) Y. J. Shen, H. X. Wang, J. D. Liu, Y. T. Zhang, *ACS Sustainable Chem. Eng.* **2015**, *3*, 1819-1829; f) Q. P. Xin, J. Y. Ouyang, T. Y. Liu, Z. Li, Z. Li, Y. C. Liu, S. F. Wang, H. Wu, Z. Y. Jiang, X. Z. Gao, *ACS Appl. Mater. Interfaces* **2015**, *7*, 1065-1077; g) J. Kim, Q. Fu, K. Xie, J. M. P. Scofield, S. E. Kentish, G. G. Qiao, *J. Membrane Sci.* **2016**, *515*, 54-62; h) G. Y. Dong, Y. T. Zhang, J. W. Hou, J. N. Shen, V. Chen, *Ind. Eng. Chem. Res.* **2016**, *55*, 5403-5414.
[93] a) C. Chen, W. S. Ahn, *Chem. Eng. J.* **2011**, *166*, 646-651; b) W. Chaikittisilp, H. J. Kim, C. W. Jones, *Energy Fuels* **2011**, *25*, 5528-5537.
[94] C. Chen, D.-W. Park, W.-S. Ahn, *Appl. Surf. Sci.* **2013**, *283*, 699-704.
[95] E. A. Roth, S. Agarwal, R. K. Gupta, *Energy Fuels* **2013**, *27*, 4129-4136.
[96] a) M. G. Plaza, C. Pevida, A. Arenillas, F. Rubiera, J. J. Pis, *Fuel* **2007**, *86*, 2204-2212; b) Y. F. Guo, C. W. Zhao, C. H. Li, S. X. Lu, *Appl. Energy* **2014**, *129*, 17-24.
[97] Z. H. Zhang, B. D. Wang, Q. Sun, L. R. Zheng, *Appl. Energy* **2014**, *123*, 179-184.
[98] R. B. Vieira, H. O. Pastore, *Environ. Sci. Technol.* **2014**, *48*, 2472-2480.
[99] a) J. T. Wang, H. C. Chen, H. H. Zhou, X. J. Liu, W. M. Qiao, D. H. Long, L. C. Ling, *J.Environ. Sci.* **2013**, *25*, 124-132; b) J. T. Wang, H. H. Huang, M. Wang, L. W. Yao, W. M. Qiao, D. H. Long, L. C. Ling, *Ind. Eng. Chem. Res.* **2015**, *54*, 5319-5327; c) J. T. Wang, M. Wang, B. B. Zhao, W. M. Qiao, D. H. Long, L. C. Ling, *Ind. Eng. Chem. Res.* **2013**, *52*, 5437-5444.
[100] X. X. Wang, C. S. Song, A. M. Gaffney, R. Z. Song, *Catal. Today* **2014**, *238*, 95-102.
[101] Y. Lin, Q. Yan, C. Kong, L. Chen, *Sci. Rep.* **2013**, *3*.
[102] H. Sehaqui, M. E. Galvez, V. Becatinni, Y. C. Ng, A. Steinfeld, T. Zimmermann, P. Tingautt, *Environ. Sci. Technol.* **2015**, *49*, 3167-3174.
[103] J. Fujiki, K. Yogo, *Energy Fuels* **2014**, *28*, 6467-6474.
[104] a) Z. Chen, S. Deng, H. Wei, B. Wang, J. Huang, G. Yu, *ACS Appl. Mater. Interfaces* **2013**, *5*, 6937-6945; b) J. T. Wang, M. Wang, W. C. Li, W. M. Qiao, D. H. Long, L. C. Ling, AlChE J. **2015**, *61*, 972-980.
[105] P. Y. Li, B. Q. Ge, S. J. Zhang, S. X. Chen, Q. K. Zhang, Y. N. Zhao, *Langmuir* **2008**, *24*, 6567-6574.
[106] a) Q. H. Wu, S. X. Chen, H. Liu, *Rsc Adv.* **2014**, *4*, 27176-27183; b) T. Xu, Q. Wu, S. Chen, M. Deng, *Rsc Adv.* **2015**, *5*, 32902-32908.
[107] F. S. Li, W. Qiu, R. P. Lively, J. S. Lee, A. A. Rownaghi, W. J. Koros, *Chemsuschem* **2013**, *6*, 1216-1223.
[108] C. H. Lee, D. H. Hyeon, H. Jung, W. Chung, D. H. Jo, D. K. Shin, S. H. Kim, *J. Ind. Eng. Chem.* **2015**, *23*, 251-256.
[109] S. Xian, F. Xu, C. Ma, Y. Wu, Q. Xia, H. Wang, Z. Li, *Chem. Eng. J.* **2015**, *280*, 363-369.
[110] R. A. Khatri, S. S. C. Chuang, Y. Soong, M. Gray, *Energy Fuels* **2006**, 20, 1514-1520.
[111] a) A. Goeppert, H. Zhang, M. Czaun, R. B. May, G. K. S. Prakash, G. A. Olah, S. R. Narayanan, *Chemsuschem* **2014**, 7, 1386-1397; b) W. B. Zhang, H. Liu, C. G. Sun, T. C. Drage, C. E. Snape, *Chem. Eng. Sci.* **2014**, 116, 306-316.

Entry for the Table of Contents, Image and Text

REVIEW

Polyethylenimine (PEI) functionalized solid adsorbents and membranes are promising for CO_2 capture and separation from flue gas or air. The review discusses the mechanism of CO_2 capture with PEI from theoretical study and summarizes the performance of CO_2 capture and separation with PEI functionalized silica, nanotubes, membranes and other low cost materials (nanosized and macrosized) from experimental work.

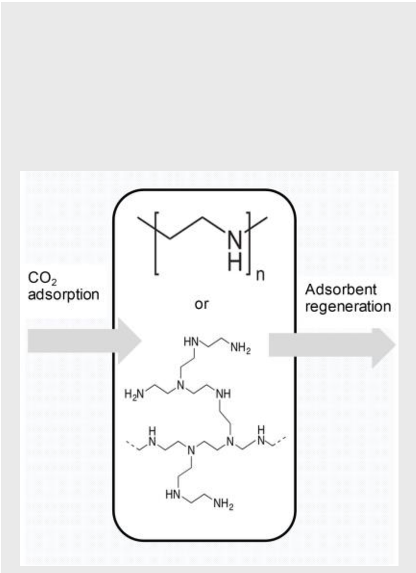

*Author(s), Corresponding Author(s)**

Xinhua Shen, Hongbo Du, Riley H. *Mullins, Raghava R. Kommalapati**

Page No. 1– Page No. 13

Title
Polyethylenimine Applications in CO_2 Capture and Separation: from Theoretical Study to Experimental Work